Induction of promyelocytic leukemia zinc finger protein by miR-200c-3p restores sensitivity to anti-androgen therapy in androgen-refractory prostate cancer and inhibits the cancer progression via down-regulation of integrin α3β4

Sadan Dahal
Yeungnam University
Prakash Chaudhary
Yeungnam University
Jung-Ae Kim (jakim@yu.ac.kr)
Yeungnam University

Research Article

Keywords: Androgen-refractory prostate cancer, Integrin α3β4, Promyelocytic leukemia zinc finger protein (PLZF), miR-200c-3p, Cancer stem cells

Posted Date: October 20th, 2022

DOI: https://doi.org/10.21203/rs.3.rs-2171149/v1

Additional Declarations: No competing interests reported.

Version of Record: A version of this preprint was published at Cellular Oncology on March 30th, 2023. See the published version at https://doi.org/10.1007/s13402-023-00803-y.

Abstract

Purpose

Androgen-refractory prostate cancer (ARPC) is one of the aggressive human cancers with metastatic capacity and resistance to androgen deprivation therapy (ADT). The present study investigated the genes responsible for ARPC progression and ADT resistance, and their regulatory mechanisms.

Methods

Transcriptome analysis, co-immunoprecipitation, confocal microscopy, and FACS analysis were performed to determine differentially-expressed genes, integrin α3β4 heterodimer, and cancer stem cell (CSC) population. miRNA array, 3'-UTR reporter assay, ChIP assay, qPCR, and immunoblotting were used to determine differentially-expressed microRNAs, their binding to integrin transcripts, and gene expressions. A xenograft tumor model was used to assess tumor growth and metastasis.

Results

Metastatic ARPC cell lines (PC-3 and DU145) exhibiting significant downregulation of *ZBTB16* and *AR* showed significantly upregulated ITGA3 and ITGB4. Silencing either one of the integrin α3β4 heterodimer significantly suppressed ARPC survival and CSC population. miRNA array and 3'-UTR reporter assay revealed that miR-200c-3p, the most strongly downregulated miRNA in ARPCs, directly bound to 3'-UTR of *ITGA3* and *ITGB4* to inhibit the gene expression. Concurrently, miR-200c-3p also increased PLZF expression, which, in turn, inhibited integrin α3β4 expression. Combination treatment with miR-200c-3p mimic and AR inhibitor enzalutamide showed synergistic inhibitory effects on ARPC cell survival *in vitro* and tumour growth and metastasis of ARPC xenografts *in vivo*, and the combination effect was greater than the mimic alone.

Conclusion

This study demonstrated that miR-200c-3p treatment of ARPC is a promising therapeutic approach to restore the sensitivity to anti-androgen therapy and inhibit tumor growth and metastasis.

1. Introduction

Prostate cancer is the second leading annual cause of cancer mortality in men worldwide [1], and the 5-year survival rate of the patients with distant metastasis remains dismal [2]. Initially, most prostate cancers respond to androgen deprivation therapy (ADT). However, ADT fails and the cancers progress to androgen-refractory state [3]. Recurrent and metastasised prostate cancer is considered castration-

resistant or androgen-refractory prostate cancer (ARPC). ARPC also develops resistance to other treatment options including bone metastasis-targeted radiopharmaceuticals [4, 5].

The promyelocytic leukaemia zinc finger (PLZF), also known as *ZBTB16*, is a zinc finger transcription factor. PLZF is widely distributed in many cell types including stem cells and progenitor cells, but its expression is higher in some tissues such as prostate than in other tissues [6]. PLZF knock-out in mouse induced several defects in musculoskeletal development and germ cell production [7, 8]. PLZF is also known to maintain self-renewal of stem cells, but the action is cell-type specific [9]. In cancers, PLZF expression level varies depending om cancer type; decrease in liver and pancreatic cancer but increase in colorectal cancer compared to normal tissue [10]. In prostate cancer, PLZF expression is inversely correlated with high grade [11]. PLZF expression is reported to be under control of AR [12], but the opposite seems to be possible: PLZF knock-down in androgen responsive prostate cancer cells (e.g, LNCaP) induces resistance to ADT and enhances androgen-independent growth of the cells [13]. Despite the various studies on the role of PLZF in cancer progression, it is still uncovered the exact regulatory mechanism on PLZF expression and its specific action in ARPC progression.

Cancer stem cells (CSCs) have the ability to self-renew and immortalise; this makes them resistant to chemo- and radiation-therapy [14, 15]. As CSCs exhibit epithelial-mesenchymal transition (EMT), recurrence, and metastasis [15–18], they are regarded as the cause of tumourigenesis, recurrence, and metastasis. Prostate tumours also contain CSCs [19], and the population is increased in patients who have received ADT [20]. Prostate CSCs (PCSCs) are also known to have no or low AR expression [21], explaining their insensitivity to androgen therapy [22]. Such PCSCs are identified by the presence of several markers, including cell surface molecules (CD44, CD133, integrins) and transcription factors (TFs) associated with stemness (Nanog, Oct4, Sox2) [21, 23]. Among the CSC markers, integrins regulate multiple stem cell functions including metastatic reactivation and chemoresistance [24–26]. Compared to normal stem cells in prostate, which express integrins α2β1 [27], PCSCs exhibit high expression of integrins α6, β1, β3, and β4, which promote self-renewal [28]. Increasing evidence suggests that integrins play an essential role in PCSC enrichment and phenotype change to ARPC after ADT. However, the mechanism underlying integrin overexpression needs to be uncovered.

MicroRNAs (miRNAs), a class of small single-stranded non-coding RNA molecules targeting about 60% of the human genes [29, 30], regulate expression of genes related to proliferation, differentiation, and apoptosis [31–34]. miRNAs in recurrent prostate cancer cells are differentially expressed compared to those in non-recurrent prostate cancer cells [35]. Differentially expressed miRNAs regulate CSC maintenance directly—by targeting CSC markers—as well as indirectly by targeting signalling molecules involved in EMT, metastasis, and drug resistance [36, 37].

In the present study, we investigated how ARPCs acquire ADT resistance and metastatic phenotype through comprehensive analysis of genes and miRNAs differentially expressed between hormone-sensitive and ARPC cells.

2. Materials And Methods

2.1. Cell culture

Human prostate cancer cell lines (LNCaP, PC-3, and DU145) and human embryonic kidney cell line (HEK-293) purchased from the Korean Cell Line Bank (Seoul, South Korea) were cultured in DMEM/High glucose (DU145) or RPMI1640 (PC-3 and LNCaP) or MEM (HEK-293) supplemented with 10% fetal bovine serum, and maintained in a humidified incubator at 37°C in a 5% CO_2 atmosphere.

2.2. Transcriptome analysis

mRNAs were extracted and analysed using the Nanostring nCounter PanCancer Progression and Cancer Pathway array kits and systems by PhilKorea (Seoul, South Korea). Genes with ≥ 2-fold change in expression ($p < 0.05$) were considered differentially expressed. The functional network of differentially expressed genes (DEGs) was analysed using STRING version 11.0 [39] or Panther classification system 16.0 [40]. In Gene Ontology (GO) enrichment analysis, pathways with false discovery rate (FDR) < 0.05 for the DEGs were considered the most significantly and differentially regulated.

2.3. Protein extraction, immunoblotting, and co-immunoprecipitation (co-IP)

Equal amounts of protein extracts were separated by SDS-PAGE, and transferred onto Hybond ECL nitrocellulose membranes (Amersham Life Science, Buckinghamshire, UK). After non-specific binding was blocked using 5% bovine serum albumin in TBST for 1 h, membranes were incubated overnight with anti-integrin β4 antibody (Cell Signalling Technology Inc. Danvers, MA, USA), or other antibodies (Abcam, Waltham, MA, USA), at 4°C. Then, the membranes were washed and incubated with horseradish peroxidase-conjugated secondary antibody. β-Actin was used as loading control. Chemiluminescence was detected using ECL reagent on a luminescent image analyser, LAS-4000 mini.

For co-IP, total proteins were lysed in IP lysis buffer (Thermo Fisher Scientific; Waltham, MA, USA).

2.4. Sphere forming assay

Prostate cancer sphere formation assay was performed as described previously [38]. Briefly, cells (3×10^3) in prEGM media (Lonza, Basel, Switzerland) were seeded an the bottom of an ultra-low attachment 24 well plate after treatment with or without siRNA or miRNA for 72 h using Lipofectamine 2000. Images of spheres were captured and only those with a diameter > 50 μm were counted.

2.5. Cell viability and proliferation assay

For the measurement of cell viability, non-target siRNA (siNT)- or siRNA-transfected cells were seeded in a 96-well plate in a serum-starved (1%) medium. For the measurement of cell proliferation, the siRNA-transfected cells were seeded in a 96-well plate in a complete medium containing 10% FBS. After 48 h, the number of viable cells was measured by MTT assay as described earlier.

2.6. Fluorescence-activated cell sorting (FACS) analysis

Cells were probed with FITC-conjugated anti-CD44 and PE-conjugated anti-CD133 antibodies for 30 min at 4°C, and then washed. FACS was performed on BD FACS Verse flow cytometer (BD Biosciences; CA, USA). Data were analysed using FlowJo software version 7.6 (Treestar; Oregon, USA). For triple-positive CSCs expressing α3 or β4, additional APC-conjugated anti-integrin α3 and PE-CY7-conjugated anti-integrin β4 antibodies were used.

2.7. miRNA array and target gene prediction

miRNAs were extracted and analyzed for differential expression using Affymetrix miRNA kit and systems (Affymetix; Santa Clara, CA, USA) by Macrogen (Seoul, South Korea). miRNAs with ≥ 2-fold change were considered differentially expressed. False discovery rate (FDR) was controlled by adjusting the *p*-value using Benjamini–Hochberg algorithm. All Statistical tests and DEG visualisation were conducted using R 3.3.2.

Target genes of differentially expressed miRNAs were predicted using TargetScan 8.0 [41].

2.8. 3'-UTR target reporter assay

HEK-293 cells were transfected with pEZX-MT05, *ITGA3*-3'-UTR, and *ITGB4*-3'-UTR purchased from GeneCopoeia Biotechnology Co. (Rockville, MD, USA). miRNA (final concentration, 50 nM) were transfected using Lipofectamine 3000 (Invitrogen). After 72 h, media were collected, luminescence was measured using Secrete-Pair Dual Luminescence Assay Kit (Genecopoeia) on FLUOstar Omega microplate reader (BMG Labtech; Ortenberg, Germany).

2.9. Confocal laser-scanning microscopy

Briefly, cells (1×10^4) cultured on a 35-millimetre glass bottom dish were fixed with 4% paraformaldehyde prepared in PBS (pH 7.4), washed, and then incubated with 1% bovine serum albumin prepared in PBST for 1 h to prevent non-specific binding. Then, the cells were incubated overnight with integrin α3 or β4 antibody solution at 4°C, and probed with fluorescence-conjugated secondary antibodies in the dark for 1 h at 25°C. Stained cells were washed and counterstained with DAPI. Images were captured at 200× magnification using a Nikon A1Si confocal microscope (Nikon Instruments Inc., Tokyo, Japan).

2.10. Chromatin immunoprecipitation (ChIP) assay, qPCR, and RT-qPCR

Chromatin extraction and subsequent ChIP assay were performed using chromatin extraction kit (Abcam) and ChIP Kit-One Step (Abcam) according to manufacturer's instructions. After chromatin cross-linking with 1% formaldehyde, chromatin was extracted and sheared by sonication. The lysates were incubated with antibodies against AR, PLZF, RNA Pol II or IgG for 2 h at 25°C. Then, proteins were digested using proteinase K, and DNA was subjected to qPCR using SYBR Green (Qiagen; Germantown, MD, USA) and primers (Bioneer; Daejeon, Korea). The primers used were *ITGA3* (Forward 5'-

GGACGTCGGTTCCCAGATGC-3' and Reverse 5'-CTCCTCATCCTCCCTACCCC-3'), *ITGB4* (5'-CTGCAGCCCATCTCCTA-3' and 5'-CCCGTCCTGGACCTACCT-3'), or *GAPDH* (5'-ACCACAGTCCATGCCATCAC-3' and 5'-TCCACCACCCTGTTGCTGTA-3'). Input DNA (1%) was used for percentage binding analysis.

For RT-PCR, mRNAs were extracted from cancer cells using TRIzol reagent, and cDNA was synthesised using GoScript Reverse Transcriptase kit (Promega Corporation, WI, USA). qPCR was performed using primers described above.

2.11. Anti-tumour and anti-metastatic activity measurements using a xenograft tumour model

The chick embryo experiments were approved beforehand by the Institutional Animal Care and Use Committee of Yeungnam University and were performed according to the guidelines issued by the Institute of Laboratory Animal Resources (1996) and Yeungnam University (The care and use of animals 2009).

On the 9th day of fertilised chicken egg incubation (37°C, 55% relative humidity), false air sac was generated on the relatively flat side of the eggs using a negative pressure technique. A small window (1 cm^2) was created on the false air sac surface, through which cancer cells (1.5×10^6 cells/CAM) labelled with cell-tracking red-florescent dye and mixed in 50% Matrigel were implanted on the exposed CAM. On the 5th day of implantation, tumour weight and vessel branch points within the tumour were analysed. For metastasis experiments, the lower CAM and liver of developing chicken embryo were collected to evaluate metastatic cells using fluorescence-aided Leica L2 microscope (Leica, Tokyo, Japan). The lower CAM and liver tissues were further analysed to detect human DNA hypoxanthine phosphoribosyltransferase (HPRT) using PCR.

2.12. Statistical analysis

One-way ANOVA followed by Student–Newman–Keuls comparison (GraphPad Prism 8.0 software; San Diego, CA, USA) was used for statistical analysis. Data are presented as means ± SEMs, and $p < 0.05$ was considered significant.

3. Results

3.1. Survival and growth of ARPC cells deficient AR and PLZF is maintained by overexpressed integrin α3 and β4

We investigated the molecules responsible for the growth of ARPC cells by comparing the gene expression levels of hormone-sensitive LNCaP and ARPC cell lines, PC-3 and DU145 [42]. Transcriptome

analysis of the total 1,333 genes revealed significantly up- and down-regulated in ARPC cell lines (compared to LNCaP cells) (Supplementary Fig. S1A). Functionally enriched pathway analysis of 147 genes that were significantly up-regulated in both PC-3 and DU145 (Supplementary Fig. S1B) showed that the genes were associated with focal adhesion, signalling receptor binding, and integrin complex/signalling pathway as well as gonadotropin releasing hormone receptor (GnRHR) (Supplementary Fig. S1C and S1D). On the other hand, the most strongly down-regulated gene in both PC-3 and DU-145 cells was *ZBTB16* (Supplementary Fig. S1A and Supplementary Table S1). The 55 genes that were commonly down-regulated in the ARPC cell lines (Supplementary Fig. S1E) were mostly associated with the GnRHR pathway and gene expression regulatory process (Supplementary Fig. S1G and S1F). The transcriptome analysis result indicates that in addition to the genes of GnRHR pathway, genes associated with integrin signalling pathway play a critical role in the ARPC cell survival and growth. Indeed, most of the integrin genes were up-regulated in ARPC cells, among which *ITGA3* and *ITGB4* were the most strongly and significantly upregulated (Table 1). Similar to the mRNA levels, the protein levels of AR and PLZF in PC-3 and DU145 cells were almost not detectable (Fig. 1A). On the other hand, integrin α3 and β4 protein expressions were strongly increased in PC-3 and DU-145 cells which also showed E-cadherin down-regulation and Snail up-regulation, corresponding to the metastatic nature of the cells (Fig. 1A). The expression level of integrin α3 and β4 in PC-3 cells was stronger than DU145 cells. We, then, examined whether integrin α3 and β4 are involved in PLZF down-regulation as well as CSC population responsible for survival and growth of ARPC cells, by silencing *ITGA3* and *ITGB4*. In silencing *ITGA3* or *ITGB4* with two different siRNA sequences in ARPC cells, siRNA sequence-2 (siRNA-2) was used throughout the experiments, as siRNA-2 of *ITGA3* and *ITGB4* was more selective (Fig. 1B). Knock-down of *ITGA3* and *ITGB4* did not change the expression level of AR and PLZF, but significantly suppressed the protein expression of CD44 and stemness-associated TFs, Sox2, Oct4 and Nanog (Fig. 1B). Consistently, *ITGA3* or *ITGB4* knockdown significantly inhibited sphere formation to the same level, regardless of differences in sphere-forming ability between ARPC and LNCaP cells (Fig. 1C). In addition, although *ITGA3* or *ITGB4* knock-down suppressed survival (Fig. 1D) and proliferation (Supplementary Fig. S1H) of PC-3 cells by more than 50%, enzalutamide did not alter the *ITGA3* or *ITGB4*-silenced cell viability, unlike non-target siRNA-treated cells.

Table 1
Integrin gene expressions with significant difference in PC-3 and DU145 cells compared to LNCaP cells

	PC-3		DU145	
	Fold Change	**p-Value**	**Fold Change**	**p-Value**
ITGA3	90.33	0.0075	57.8	0.0103
ITGB4	81.03	0.0118	12.14	0.0491
ITGB8	23.27	0.0461	2.59	0.3655
ITGA2	15.0	0.0436	7.21	0.0701
ITGB3	5.74	0.0329	4.61	0.0460
ITGB2	5.53	0.0127	6.55	0.0050
ITGA1	4.35	0.0003	3.66	0.0100
ITGB1	4.35	0.0017	4.66	0.0002
ITGA6	4.27	0.0010	4.12	0.0002
ITGB6	1.97	0.4093	1.56	0.6780
ITGA7	1.83	0.1957	3.37	0.0872
ITGA5	1.58	0.3178	4.39	0.0461
ITGA9	1.43	0.6635	3.85	0.1786
ITGB7	1.11	0.7013	-2.07	0.0989
ITGA11	-1.2	0.6953	2.1	0.1627
ITGA8	-2.2	0.5246	2.34	0.4336

Because integrins normally function as a αβ heterodimer, we investigated whether integrins α3 and β4 form a heterodimer. The co-IP result revealed that integrin α3 bound to β4, forming a heterodimer in PC-3 cells (Fig. 2A). In addition, the population of $CD44^+CD133^+$ PCSC population in ARPC cells was similar to that of $CD44^+CD133^+\alpha3^+$ or $CD44^+CD133^+\beta4^+$, indicating that PCSCs expressed integrin α3 and β4 (Fig. 2B). Consistent to the sphere forming ability, the PCSC $CD44^+CD133^+\alpha3^+$ or $CD44^+CD133^+\beta4^+$ population counts were higher in PC-3 than in DU145 (Fig. 2B). Nonetheless, silencing either *ITGA3* or *ITGB4* completely abolished $CD44^+CD133^+$ PCSC in both PC-3 and DU-145 cells (Fig. 2C), suggesting that α3β4 heterodimer was critical for the PCSC maintenance.

3.2. Differentially expressed miRNAs regulate androgen-refractory genes (AR and PLZF) and integrin α3β4 in ARPC cell lines

Next, we investigated that the most significantly down-regulated *AR* and *PLZF* are involved in the up-regulation of *ITGA3* and *ITGB4.* Along with differentially up-regulated *ITGA3* and *ITGB4*, the top three down-regulated genes were *ZBTB16*, *KLK3*, and *TMPRSS2* (Supplementary Table S1). Although these genes are under direct transcriptional regulation of AR [10, 43], the relative expression of the three genes in ARPC cells was lower than that of AR (Supplementary Table S1), implicating molecules other than AR may be involved in down-regulation of the genes. To elucidate the involvement of miRNAs as master regulatory molecules associated with these gene expressions, miRNA array was performed. Among the total 2,578 mature miRNAs, 184 and 314 miRNAs were differentially expressed in PC-3 and DU145 cells, respectively (compared to LNCaP cells) (Fig. 3A). The top two upregulated miRNAs in PC-3 and DU145 cells were miR-130a-3p and miR-29b-1-5p, while the top two downregulated miRNAs in PC-3 and DU145 cells were miR-200c-3p and miR-99a-5p in PC-3 versus miR-99a-5p and miR-148a-3p in DU145 (Fig. 3B, Supplementary Table S2). In case of miR-148a-3p, relative expression in PC-3 and DU145 was similar (Supplementary Table S2). For the five miRNAs, putative target genes were predicted using TargetScan [44, 45]. miR-130a-3p and miR-29b-1-5p showed negative correlation with *ZBTB16* and *AR* transcripts (Table 2). In contrast, miR-200c-3p and miR-148a-3p showed a positive correlation with *ZBTB16*, whereas miR-99a-5p showed no correlation with either *ZBTB16* or *AR* as target genes in ARPC cells (Table 2). Accordingly, we focused on four miRNAs and further examined their interaction with highly up- and down-regulated genes. Bioinformatic analysis revealed that the 3'-UTR of *ITGA3* and *ITGB4* contained putative binding sites for the four miRNAs (Supplementary Fig. S2). However, the 3'-UTR reporter gene assay revealed that only the miR-200c-3p mimic significantly repressed the normalised luciferase activity of *ITGA3* and *ITGB4* reporter genes (Fig. 3C). In case of miR-148 mimic treatment, inhibition of the reporter gene activity was weak, and the mix of the four different miRNA mimics exhibited similar effect on the 3'-UTR of *ITGA3* as the miR-200c-3p mimic. Likewise, the mix of the four different miRNA inhibitors did not alter the 3'-UTR reporter luciferase activity. Such regulatory activity of miR-200c-3p was also confirmed by mRNA (Fig. 3D) and protein (Fig. 3E, Supplementary Fig. S3A) expressions of integrin α3β4 in both LNCaP and PC-3 cells. The changes in α3β4 expression levels by miR-200c-3p mimic and inhibitors were also confirmed by fluorescence microscopy (Fig. 3F). Importantly, PLZF and AR were up- and downregulated by the miR-200c-3p mimic and inhibitor, respectively (Fig. 3D and 3E). Corresponding to those gene expression changes, spheroid formation was significantly inhibited by the miR-200c-3p mimic, but significantly increased by miR-200c-3p inhibitor in both LNCaP and ARPC cell lines (Fig. 3G).

Table 2

Differentially expressed miRNAs and their predicted target genes selected from DEGs commonly up- and down-regulated in PC-3 and DU145 cells (Fold Change ≥ 2, $p < 0.05$)

Upregulated miRNA	Corresponding targets among commonly changed DEGs in PC-3 and DU145 cells[a]		Downregulated miRNA	Corresponding targets among commonly changed DEGs in PC-3 and DU145 cells[a]	
miR-130a-3p	Up	ARAP2, CEP170, CREB5, ELK3, EPHB4, EREG, F3, FERMT2, FOSL1, KIAA1462, MET, NFATC2, PPARG, SERPINH1, SLC2A1, SMURF2, TGFB2, TGFBR2	miR-200c-3p	Up	AHNAK, AKAP2, BICC1, CBL, CREB5, CYP1B1, ELK3, ETS2, FERMT2, IRS1, KIAA1462, LHFP, LOX, PIK3CA, PRKCA, SLIT2, SMURF2
	Down	AR, BMPR2, BTG1, CDKN1A, ERBB3, MAF, PRKACB, TBL1XR1, ZBTB16		Down	GATA2, MAF, PRKACB, TBL1XR1, ZBTB16
miR-29b-1-5p	Up	AKAP12, AKAP2, AKT3, ARAP2, BDNF, CD44, CDC25B, CDK6, CLCF1, CREB5, EGFR, HMGA2, IRS1, ITGA1, ITGB2, KIAA1462, KITLG, LAMC2, LIF, MECOM, MET, MMP14, MSH2, PDGFC, PIK3CA, PLCG2, PLS1, PRKCA, RUNX1, TFPI2, TGFB2, THBS1, TNC, VEGFC	miR-148a-3p	Up	ARAP2, BICC1, CDC25B, CDK6, COL4A1, EGFR, EPAS1, F3, FGF2, HMGA2, MET, PIK3CA, SLC2A1, SMURF2, SOS1, TGFB2
				Down	ERBB3, MAF, NCOR1, PIK3R3, TBL1XR1, ZBTB16

[a]The corresponding target genes were predicted using TargetScan.

Upregulated miRNA	Corresponding targets among commonly changed DEGs in PC-3 and DU145 cells[a]		Downregulated miRNA	Corresponding targets among commonly changed DEGs in PC-3 and DU145 cells[a]	
	Down	AR, CACNA1D, CEBPA, CTSH, FANCF, GRHL2, PIK3CD, PIK3R3, PLCB4, PPP3CA, SORD, TBL1XR1, ZBTB16	miR-99a-5p	Up	Not available
				Down	PPP3CA, BMPR2

[a]The corresponding target genes were predicted using TargetScan.

3.3. Both miR-200c-3p and miR-200c-3p-induced PLZF suppress integrin α3β4 expression

As upregulation of integrin α3 and β4 by miR-200c-3p inhibitor was accompanied by downregulation of AR and PLZF, we examined whether miR-200c-3p-regulated PLZF was also involved in the expression of α3 and β4. In case of ChIP-qPCR with anti-AR antibody, there was no binding of AR to the integrin genes, whereas with anti-PLZF antibody it showed that PLZF directly bound to the *ITGA3* and *ITGB4* promoter in both LNCaP and PC-3 cells, with greater binding affinity to *ITGA3* than to *ITGB4* (Fig. 4A). Notably, PLZF binding to the genes was significantly increased by miR-200c-3p mimic (Fig. 4A). We then examined the enhanced binding of PLZF to *ITGA3* and *ITGB4* promoter induce down regulation of integrin α3β4 by comparing the effect of *PLZF* siRNA, miR-200c-3p, and combination of the two. Treatment of cells with miR-200c-3p mimic strongly enhanced *PLZF* expression, but suppressed the expression of *ITGA3* (Fig. 4C) and *ITGB4* (Fig. 4D). In contrast, miR-200c-3p inhibitor suppressed *PLZF* expression, but increased the expression of *ITGA3* and *ITGB4*. The degree of *PLZF* suppression by miR-200c-3p inhibitor was similar to that by *PLZF* siRNA (Fig. 4B). The effects of *PLZF* siRNA on the gene expressions were offset by co-treatment with miR-200c-3p mimic, but synergistically enhanced by co-treatment with miR-200c-3p inhibitor (Fig. 4B-4D). The pattern of the gene expression changes was identical to that of stemness-associated TFs, Sox2, Oct4 and Nanog (Fig. 4E and Supplementary Fig S3B). The effects of *PLZF* siRNA, miR-200c-3p mimic/inhibitor, or combination of the two on integrin α3β4 expression co-localised in the plasma membrane were further confirmed by confocal microscopy (Fig. 4F). Corresponding to the restoration of PLZF expression by miR-200c-3p mimic, the decrease in cell viability by 200c-3p mimic was further enhanced by co-treatment with enzalutamide in a concentration-dependent manner, resulting in complete reduction of PC-3 cell viability (Fig. 4G). Corresponding to the α3β4 and PLZF expression changes, the population counts of PCSCs that also express α3 (Fig. 5A) and β4 (Fig. 5B) were completely suppressed by miR-200c-3p mimic. In contrast, 200c-3p inhibitor that induced PLZF down-regulation increased synergistically enhanced the PCSC population upon co-treatment with PLZF siRNA.

3.4. miR-200c-3p mimic restores androgen sensitivity and inhibits tumour growth and metastasis of implanted PC-3 cells in a xenografted tumour model.

We further examined the anti-cancer effect of miR-200c-3p mimic against ARPC using xenograft CAM tumour model. Tumour growth and tumour-induced angiogenesis in PC-3 xenografts was greater than that in LNCaP xenografts (Fig. 6A). Treatment with miR-200c-3p mimic (1.5 pmole/CAM) significantly inhibited tumour growth and angiogenesis in both LNCaP and PC-3 implants (Fig. 6B). Enzalutamide (300 pmole/CAM) inhibited tumour growth of LNCaP xenograft, but not PC-3 xenograft (Fig. 6B). However, when enzalutamide was co-administered with miR-200c-3p mimic, the growth of PC-3 xenografts was synergistically inhibited, and the effect was greater than that of miR-200c-3p mimic alone (Fig. 6B). Moreover, unlike LNCaP implants with non-detectable metastasis, PC-3 implants significantly metastasised to the developing chick liver and to the bottom side CAM (Fig. 6C). Importantly, metastasis of PC-3 xenografts to the liver and lower CAM was completely blocked by miR-200c-3p mimic alone as well as co-treatment with miR-200c-3p mimic and enzalutamide (Fig. 6D).

4. Discussion

Here, we demonstrated the mechanism by which prostate cancer acquires resistance and metastatic potentials. Integrin α3β4 overexpressed in ARPC cells were functional as a heterodimer for PCSC maintenance, and the gene expression was suppressed by both transcription factor PLZF and miR-200c-3p. Notably, PLZF itself expression was induced by miR-200c-3p. By restoring miR-200c-3p level, which was the most strongly decreased in ARPCs, sensitivity to anti-androgen therapy was recovered in ARPCs, and the growth and metastasis of ARPC tumors were greatly suppressed.

Transcriptome analysis revealed that highly metastatic ARPC cells expressed significantly higher level of integrins than LNCaP; integrin α3β4 expression being the highest. Studies have shown that prostate primary tumour CSCs expressing integrin $\alpha2\beta1^{high}$ are more invasive than the cells not expressing α2β1 [46, 47]. Metastatic ARPCs with up-regulation of α2β1, and much higher expression of α3β4 levels than α2β1, correlated with the degree of CSC enrichment in ARPCs. As integrins regulate maintenance of CSCs contributing to cancer progression and heterogeneity [48, 49], α3β4 silencing in the present study resulted in significant decrease in CSC counts, consequently, tumour growth and metastasis of ARPCs. Consistent with previous reports [28, 50, 51], our results also indicate that prostate cancer aggressiveness was dependent on the expression of integrin β4. Additionally, our results revealed integrin α3 upregulation in ARPC, highlighting its important role in prostate cancer aggressiveness and transformation into ARPC. Notably, unlike normal prostate stem cells in which integrin β4 is tightly associated with α6 [52], our study revealed that integrin β4 also work together with α3 in metastatic ARPCs. Integrin α6 expression was much less than β4, whereas α3 expression was more than enough to form dimer with β4 in PC and DU145, as demonstrated by co-IP. More importantly, silencing either α3 or β4 inhibited expression of both α3 and β4 along with complete suppression of CSC formation, indicating that α3 and β4 were mutually inter-regulated by each other, and that α3β4 complex was the major player in maintaining prostate CSCs.

Although a cross-talk existed between integrin α3 and β4, the major regulator of α3β4 expression was miR-200c-3p. miR-200c-3p binds directly to the 3'-UTR of integrin α3β4, resulting in post-transcriptional repression, in spite of the fact that no canonical binding site was predicted in the 3'-UTR of integrin α3 or β4 that matched the miR-200c-3p seed region. Rather, compensatory pairing sites were centered at 13–17th miRNA nucleotides at the 5' end and extended more than five contiguous Watson–Crick pairs [53]. Regardless of canonical or compensatory sites, the pairing and binding of miRNA to target mRNA causes post-transcriptional repression [30], which was further proved in the present study through down- and up-regulation of the genes by miR-200c-3p mimic and inhibitor, respectively.

Another way via which miR-200c-3p regulated α3β4 expression involved PLZF, which binds to α3β4 DNA and represses transcription of these genes. As a transcription repressor, PLZF exhibited greater capacity to bind α3 than to β4. 200c-3p mimic up-regulated both AR and PLZF, but only PLZF was involved in α3β4 gene expression. Interestingly, stringent seed pairing predicted PLZF as one of the target genes of both upregulated miRNAs (miR-130a-3p and miR-29b-1-5p) and downregulated miRNAs (miR-200c-3p and miR-148a-3p), which did not follow classical miRNA actions, i.e., translational repression or mRNA degradation. Rather, regulation of PLZF expression by miR-200c-3p seemed to involve recently discovered miRNA functions, such as post-transcriptional upregulation of target genes through direct and indirect mechanisms, ligand for cell surface receptors, or nuclear transcription factor activator [54–56]. 3'-UTR reporter assay and ChIP-qPCR confirmed that miR-200c-3p performed a dual regulatory action in α3β4 expression, i.e., PLZF-mediated and direct binding to the genes.

Concurrent with the correlation between PLZF levels and inhibition of prostate cancer proliferation [12, 57, 58], our *in vivo* results confirmed that tumour growth of PC-3 xenografts with non-detectable PLZF was greater than that of LNCaP xenografts with more PLZF. Further, the miR-200c-3p mimic inhibited the growth of enzalutamide-insensitive PC-3 xenografts to the same extent as that of LNCaP xenografts. Despite the anti-tumour activity of miR-200c-3p being proven in prostate cancer [59], our study provides more detailed mechanism by which reduced miR-200c-3p levels induce anti-androgen resistance and metastasis *in vivo*. In both LNCaP and PC-3 xenografts, the effect of combination treatment with miR-200c-3p mimic and enzalutamide on the tumour growth was much greater than that of miR-200c-3p mimic or enzalutamide alone. More importantly, miR-200c-3p mimic almost completely inhibited metastasis of PC-3 xenografts, indicating the excellency in the therapeutic efficacy of miR-200c-3p in ARPC.

In conclusion, in metastatic ARPC cells, integrin α3β4 expression was strongly increased along with PLZF and AR downregulation (resulting from downregulation of miR-200c-3p). Integrin α3β4 expression was inhibited by both miR-200c-3p and miR-200c-3p-induced PLZF. Restoring miR-200c-3p levels with its mimic greatly inhibited ARPC progression, *in vivo* tumour growth and metastasis, through PLZF recovery and α3β4 suppression.

Abbreviations

ADT, Androgen deprivation therapy; ARPC, Androgen-refractory prostate cancer; CSCs, Cancer stem cells; DEGs, Differentially expressed genes; EMT, Epithelial-mesenchymal transition; FACS, Fluorescence-activated cell sorting; FDR, False discovery rate; GO, Gene Ontology; HPRT, hypoxanthine phosphoribosyltransferase; siNT, Non-target siRNA; PCSCs, Prostate CSCs; PLZF, Promyelocytic leukaemia zinc finger; TFs, Transcription factors

Declarations

Acknowledgements

We would like to thank Dr. Guragain Diwakar for helping us using GO analysis program, and Editage (www.editage.co.kr) for English language editing.

Conflict of Interest

The authors have no conflict of interest to declare.

Ethical Approval

The chick embryo experiments were approved beforehand by the Institutional Animal Care and Use Committee of Yeungnam University and were performed according to the guidelines issued by the Institute of Laboratory Animal Resources (1996) and Yeungnam University (The care and use of animals 2009). (Approval number: 2022-021).

Competing Interest

There are no conflicts of interest.

Authors' contributions

Sadan Dahal: Acquisition of data, Analysis and interpretation of data, contribution to the manuscript preparation. Prakash Chaudhary: Acquisition of data, Analysis and interpretation of data, contribution to the manuscript preparation. Jung-Ae Kim: Study supervision, Conceptualization, Funding acquisition, Data curation, Writing original draft and editing. All authors have read and agreed to the manuscript.

Sadan Dahal and Prakash Chaudhary equally contributed to this work.

Funding

This work was supported by the National Research Foundation of Korea (NRF) grants funded by the Korea government (MIST) (Grant No.: NRF-2020R1A2C2005690).

Availability of data and materials

Not applicable

References

1. F. Bray, J. Ferlay, I. Soerjomataram, R.L. Siegel, L.A. Torre and A. Jemal, Global cancer statistics 2018: GLOBOCAN estimates of incidence and mortality worldwide for 36 cancers in 185 countries. CA: Cancer J. Clin. **68**, 394-424 (2018)
2. R.L. Siegel, K. D. Miller, A. Jemal, Cancer statistics, 2020. CA: Cancer J. Clin. **70**, 7-30 (2020) doi: https://doi.org/10.3322/caac.21590
3. A. Hobisch, Z. Culig, C. Radmayr, G. Bartsch, H. Klocker and A. Hittmair, Androgen receptor status of lymph node metastases from prostate cancer. Prostate **28**, 129-135 (1996)
4. S. Roychowdhury and A.M. Chinnaiyan, Advancing precision medicine for prostate cancer through genomics. J. Clin. Oncol. **31**, 1866 (2013)
5. M. Nakazawa, C. Paller and N. Kyprianou, Mechanisms of therapeutic resistance in prostate cancer. Curr. Oncol. Rep. **19**, 1-12 (2017)
6. M. Uhlén, E. Björling, C. Agaton, C.A.-K. Szigyarto, B. Amini, E. Andersen, A.-C. Andersson, P. Angelidou, A. Asplund and C. Asplund, A human protein atlas for normal and cancer tissues based on antibody proteomics. Mol. Cell. Proteomics **4**, 1920-1932 (2005)
7. F.W. Buaas, A.L. Kirsh, M. Sharma, D.J. McLean, J.L. Morris, M.D. Griswold, D.G. de Rooij and R.E. Braun, Plzf is required in adult male germ cells for stem cell self-renewal. Nat. Genet. **36**, 647-652 (2004)
8. J.A. Costoya, R.M. Hobbs, M. Barna, G. Cattoretti, K. Manova, M. Sukhwani, K.E. Orwig, D.J. Wolgemuth and P.P. Pandolfi, Essential role of Plzf in maintenance of spermatogonial stem cells. Nat. Genet. **36**, 653-659 (2004)
9. A.M. Beaulieu and D.B. Sant'Angelo, The BTB-ZF family of transcription factors: key regulators of lineage commitment and effector function development in the immune system. J. Immunol. **187**, 2841-2847 (2011)
10. Y. Jin, H.Z. Nenseth and F. Saatcioglu, Role of PLZF as a tumor suppressor in prostate cancer. Oncotarget **8**, 71317 (2017)
11. G.-Q. Xiao, P. Unger, Q. Yang, Y. Kinoshita, K. Singh, L. McMahon, K. Nastiuk, K. Sha, J. Krolewski and D. Burstein, Loss of PLZF expression in prostate cancer by immunohistochemistry correlates with tumor aggressiveness and metastasis. PloS One **10**, e0121318 (2015)
12. T. Kikugawa, Y. Kinugasa, K. Shiraishi, D. Nanba, K.i. Nakashiro, N. Tanji, M. Yokoyama and S. Higashiyama, PLZF regulates Pbx1 transcription and Pbx1–HoxC8 complex leads to androgen-independent prostate cancer proliferation. Prostate **66**, 1092-1099 (2006)
13. G.-Q. Xiao, F. Li, J. Findeis-Hosey, O. Hyrien, P.D. Unger, L. Xiao, R. Dunne, E.S. Kim, Q. Yang and L. McMahon, Down-regulation of cytoplasmic PLZF correlates with high tumor grade and tumor aggression in non–small cell lung carcinoma. Hum. Pathol. **46**, 1607-1615 (2015)
14. L.T.H. Phi, I.N. Sari, Y.-G. Yang, S.-H. Lee, N. Jun, K.S. Kim, Y.K. Lee and H.Y. Kwon, Cancer stem cells (CSCs) in drug resistance and their therapeutic implications in cancer treatment. Stem Cells Int. **2018**,

(2018)

15. S. Skvortsov, I.-I. Skvortsova, D.G. Tang and A. Dubrovska, Concise review: prostate cancer stem cells: current understanding. Stem Cells **36**, 1457-1474 (2018)
16. C. Liu and D.G. Tang, MicroRNA Regulation of Cancer Stem CellsmiRNA and Cancer Stem Cells. Cancer Res. **71**, 5950-5954 (2011)
17. H. Easwaran, H.-C. Tsai and S.B. Baylin, Cancer epigenetics: tumor heterogeneity, plasticity of stem-like states, and drug resistance. Mol. Cell. **54**, 716-727 (2014)
18. J.J. Li and M.M. Shen, Prostate stem cells and cancer stem cells. C. S. H. Perspect. Med. **9**, a030395 (2019)
19. H. Li and D.G. Tang, Prostate cancer stem cells and their potential roles in metastasis. J. Surg. Oncol. **103**, 558-562 (2011)
20. S.O. Lee, Z. Ma, C.-R. Yeh, J. Luo, T.-H. Lin, K.-P. Lai, S. Yamashita, L. Liang, J. Tian and L. Li, New therapy targeting differential androgen receptor signaling in prostate cancer stem/progenitor vs. non-stem/progenitor cells. J. Mol. Cell Biol. **5**, 14-26 (2013)
21. K. Zhang, S. Zhou, L. Wang, J. Wang, Q. Zou, W. Zhao, Q. Fu and X. Fang, Current stem cell biomarkers and their functional mechanisms in prostate cancer. Int. J. Mol. Sci. **17**, 1163 (2016)
22. G. Civenni, D. Albino, D. Shinde, R. Vázquez, J. Merulla, A. Kokanovic, S.N. Mapelli, G.M. Carbone and C.V. Catapano, Transcriptional reprogramming and novel therapeutic approaches for targeting prostate cancer stem cells. Front. Oncol. **9**, 385 (2019)
23. J.P. Medema, Cancer stem cells: the challenges ahead. Nat. Cell Biol. **15**, 338-344 (2013)
24. L. Seguin, J.S. Desgrosellier, S.M. Weis and D.A. Cheresh, Integrins and cancer: regulators of cancer stemness, metastasis, and drug resistance. Trends Cell Biol. **25**, 234-240 (2015)
25. B. Bierie, S.E. Pierce, C. Kroeger, D.G. Stover, D.R. Pattabiraman, P. Thiru, J. Liu Donaher, F. Reinhardt, C.L. Chaffer and Z. Keckesova, Integrin-β4 identifies cancer stem cell-enriched populations of partially mesenchymal carcinoma cells. Proc. Natl. Acad. Sci. U. S. A. **114**, E2337-E2346 (2017)
26. J. Cooper and F.G. Giancotti, Integrin signaling in cancer: mechanotransduction, stemness, epithelial plasticity, and therapeutic resistance. Cancer Cell **35**, 347-367 (2019)
27. A.T. Collins, F.K. Habib, N.J. Maitland and D.E. Neal, Identification and isolation of human prostate epithelial stem cells based on α2β1-integrin expression. J. Cell Sci. **114**, 3865-3872 (2001)
28. T. Yoshioka, J. Otero, Y. Chen, Y.-M. Kim, J.A. Koutcher, J. Satagopan, V. Reuter, B. Carver, E. De Stanchina and K. Enomoto, β4 Integrin signaling induces expansion of prostate tumor progenitors. J. Clin. Invest. **123**, 682-699 (2013)
29. R.C. Friedman, K.K.-H. Farh, C.B. Burge and D.P. Bartel, Most mammalian mRNAs are conserved targets of microRNAs. Genome Res. **19**, 92-105 (2009)
30. Y. Peng and C.M. Croce, The role of MicroRNAs in human cancer. Signal Transduct. Target. Ther. **1**, 1-9 (2016)

31. S. Mishra, T. Yadav and V. Rani, Exploring miRNA based approaches in cancer diagnostics and therapeutics. Crit. Rev. Oncol. Hemat. **98**, 12-23 (2016)
32. A. Esquela-Kerscher and F.J. Slack, Oncomirs—microRNAs with a role in cancer. Nat. Rev. Cancer. **6**, 259-269 (2006)
33. J. Lu, G. Getz, E.A. Miska, E. Alvarez-Saavedra, J. Lamb, D. Peck, A. Sweet-Cordero, B.L. Ebert, R.H. Mak and A.A. Ferrando, MicroRNA expression profiles classify human cancers. Nature **435**, 834-838 (2005)
34. R. Kanwal, A.R. Plaga, X. Liu, G.C. Shukla and S. Gupta, MicroRNAs in prostate cancer: Functional role as biomarkers. Cancer Lett. **407**, 9-20 (2017)
35. E. Pashaei, E. Pashaei, M. Ahmady, M. Ozen and N. Aydin, Meta-analysis of miRNA expression profiles for prostate cancer recurrence following radical prostatectomy. PloS One **12**, e0179543 (2017)
36. V. Huang, R.F. Place, V. Portnoy, J. Wang, Z. Qi, Z. Jia, A. Yu, M. Shuman, J. Yu and L.-C. Li, Upregulation of Cyclin B1 by miRNA and its implications in cancer. Nucleic Acids Res. **40**, 1695-1707 (2012)
37. Y.-X. Fang, Y.-L. Chang and W.-Q. Gao, MicroRNAs targeting prostate cancer stem cells. Exp. Biol. Med. **240**, 1071-1078 (2015)
38. E.-J. Yun, J. Zhou, C.-J. Lin, E. Hernandez, L. Fazli, M. Gleave and J.-T. Hsieh, Targeting Cancer Stem Cells in Castration-Resistant Prostate CancerProstate Cancer Stem Cell Therapy. Clin. Cancer Res. **22**, 670-679 (2016)
39. D. Szklarczyk, J.H. Morris, H. Cook, M. Kuhn, S. Wyder, M. Simonovic, A. Santos, N.T. Doncheva, A. Roth and P. Bork, The STRING database in 2017: quality-controlled protein–protein association networks, made broadly accessible. Nucleic Acids Res. **45**, gkw937 (2016)
40. H. Mi, D. Ebert, A. Muruganujan, C. Mills, L.-P. Albou, T. Mushayamaha and P.D. Thomas, PANTHER version 16: a revised family classification, tree-based classification tool, enhancer regions and extensive API. Nucleic Acids Res. **49**, D394-D403 (2021)
41. S.E. McGeary, K.S. Lin, C.Y. Shi, T.M. Pham, N. Bisaria, G.M. Kelley and D.P. Bartel, The biochemical basis of microRNA targeting efficacy. Science **366**, eaav1741 (2019)
42. E. Tsakalozou, A.M. Eckman and Y. Bae, Combination effects of docetaxel and doxorubicin in hormone-refractory prostate cancer cells. Biochem. Res. Int. **2012**, (2012)
43. J.R. Olsen, W. Azeem, M.R. Hellem, K. Marvyin, Y. Hua, Y. Qu, L. Li, B. Lin, X.-S. Ke and A.M. Øyan, Context dependent regulatory patterns of the androgen receptor and androgen receptor target genes. BMC Cancer **16**, 1-15 (2016)
44. B.P. Lewis, C.B. Burge and D.P. Bartel, Conserved seed pairing, often flanked by adenosines, indicates that thousands of human genes are microRNA targets. Cell **120**, 15-20 (2005)
45. V. Agarwal, G.W. Bell, J.-W. Nam and D.P. Bartel, Predicting effective microRNA target sites in mammalian mRNAs. Elife **4**, e05005 (2015)

46. A.T. Collins, P.A. Berry, C. Hyde, M.J. Stower and N.J. Maitland, Prospective identification of tumorigenic prostate cancer stem cells. Cancer Res. **65**, 10946-10951 (2005)
47. J.K. Rane, M. Scaravilli, A. Ylipää, D. Pellacani, V.M. Mann, M.S. Simms, M. Nykter, A.T. Collins, T. Visakorpi and N.J. Maitland, MicroRNA expression profile of primary prostate cancer stem cells as a source of biomarkers and therapeutic targets. Eur. Urol. **67**, 7-10 (2015)
48. H. Hamidi, M. Pietilä and J. Ivaska, The complexity of integrins in cancer and new scopes for therapeutic targeting. Brit. J. Cancer **115**, 1017-1023 (2016)
49. J.K. Mouw, Y. Yui, L. Damiano, R.O. Bainer, J.N. Lakins, I. Acerbi, G. Ou, A.C. Wijekoon, K.R. Levental and P.M. Gilbert, Tissue mechanics modulate microRNA-dependent PTEN expression to regulate malignant progression. Nature Med. **20**, 360-367 (2014)
50. I. Rabinovitz and A.M. Mercurio, The integrin α6β4 functions in carcinoma cell migration on laminin-1 by mediating the formation and stabilization of actin-containing motility structures. J. Cell Biol. **139**, 1873-1884 (1997)
51. R.L. Stewart and K.L. O'connor, Clinical significance of the integrin α6β4 in human malignancies. Lab. Invest. **95**, 976-986 (2015)
52. S.H. Lang, E. Anderson, R. Fordham and A.T. Collins, Modeling the prostate stem cell niche: an evaluation of stem cell survival and expansion in vitro. Stem Cells Dev. **19**, 537-546 (2010)
53. D.P. Bartel, MicroRNAs: target recognition and regulatory functions. Cell **136**, 215-233 (2009)
54. S. Vasudevan, Posttranscriptional upregulation by microRNAs. Wiley Interdiscip. Rev. RNA **3**, 311-330 (2012)
55. M. Fabbri, A. Paone, F. Calore, R. Galli, E. Gaudio, R. Santhanam, F. Lovat, P. Fadda, C. Mao and G.J. Nuovo, MicroRNAs bind to Toll-like receptors to induce prometastatic inflammatory response. Proc. Natl. Acad. Sci. U. S. A. **109**, E2110-E2116 (2012)
56. S. He, J. Chu, L.-C. Wu, H. Mao, Y. Peng, C.A. Alvarez-Breckenridge, T. Hughes, M. Wei, J. Zhang and S. Yuan, MicroRNAs activate natural killer cells through Toll-like receptor signaling. Blood **121**, 4663-4671 (2013)
57. F. Jiang and Z. Wang, Identification and characterization of PLZF as a prostatic androgen-responsive gene. Prostate **59**, 426-435 (2004)
58. J. Cao, S. Zhu, W. Zhou, J. Li, C. Liu, H. Xuan, J. Yan, L. Zheng, L. Zhou and J. Yu, PLZF mediates the PTEN/AKT/FOXO3a signaling in suppression of prostate tumorigenesis. PloS One **8**, e77922 (2013)
59. J. Zhang, H. Zhang, Y. Qin, C. Chen, J. Yang, N. Song and M. Gu, MicroRNA-200c-3p/ZEB2 loop plays a crucial role in the tumor progression of prostate carcinoma. Ann. Transl. Med. **7**, (2019)

Figures

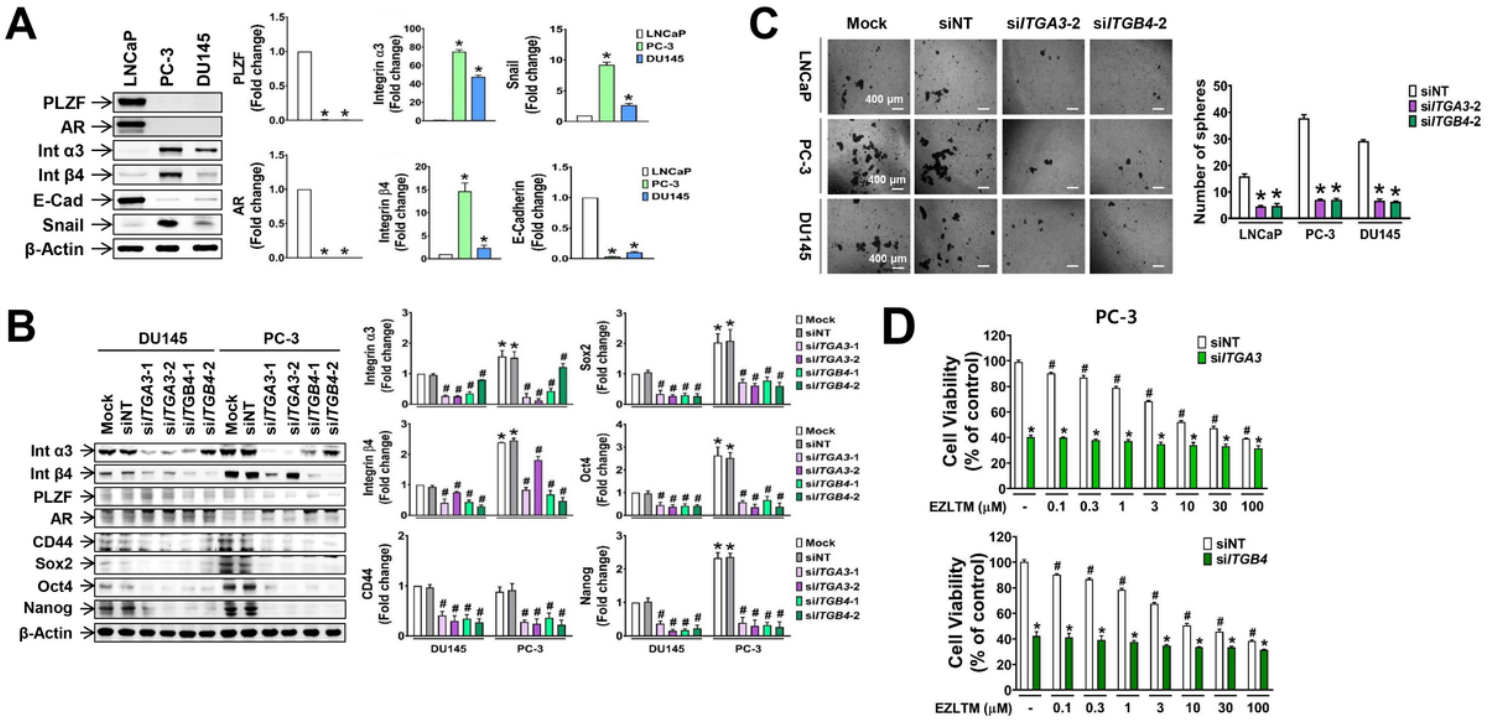

Figure 1

Up-regulated integrin α3 and β4 in ARPC cells maintains the CSC population and cell survival. (A) Immunoblots for selected genes, PLZF, AR, integrin α3, integrin β4, and E-cadherin, showing the difference in LNCaP versus ARPC cells (DU145 and PC-3). *p< 0.05, compared to LNCaP. (B) Immunoblots showing the effect of *ITGA3* or *ITGB4* knockdown on the expression of integrins and stemness marker proteins (CD44, Sox2, Oct4, and Nanog). Cells were treated with siRNA (100 nM) against *ITGA3* or *ITGB4*. Two different sequences of each siRNA were used to check specificity. The bar graphs represent the means ± SEM from three independent experiments. (C) Spheroid formation was inhibited by silencing *ITGA3* or *ITGB4*. Scale bar (white coloured) represents 400 μm at original magnification of 4×. The bar graph represents the number of spheroids over 50 μm in diameter. *p< 0.05, compared to siNT-treated control in each cell line. (D) Effects of silencing *ITGA3* or *ITGB4* on PC-3 cell viability in the absence and presence of enzalutamide. *p< 0.05, compared to siNT-treated control. $^{\#}p$<0.05, compared to vehicle-treated group.

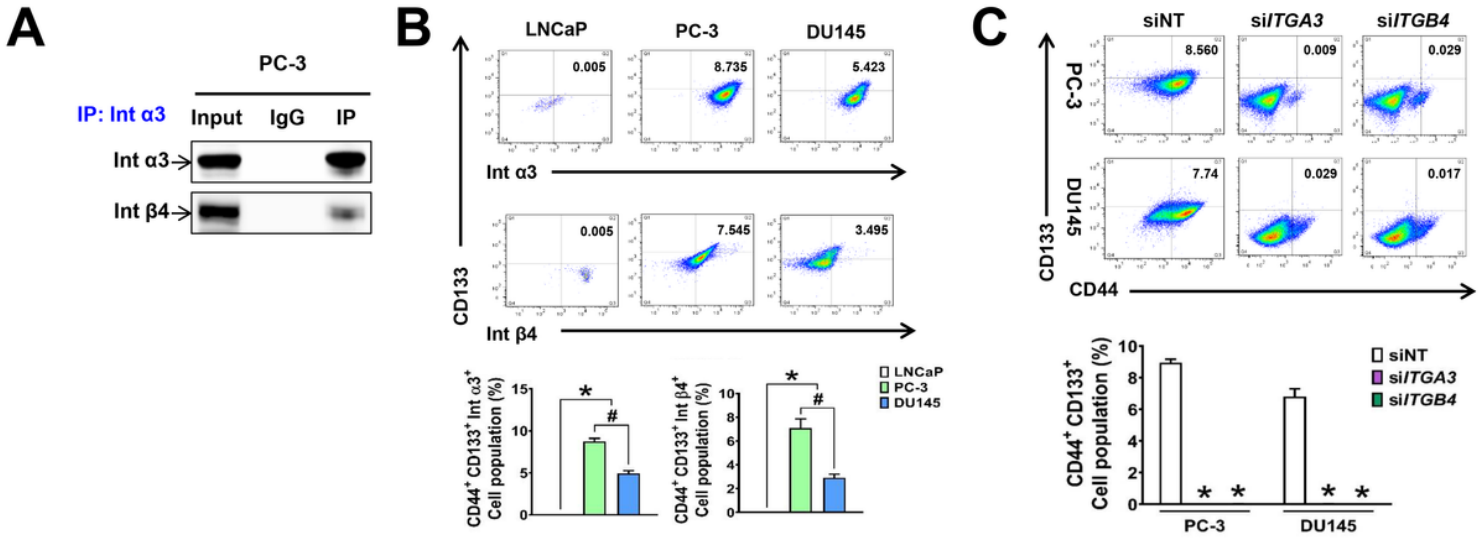

Figure 2

Integrin α3 and β4 dimer formation is critical for prostate cancer stem cell maintenance. (A) Co-IP of integrin α3 and β4 in PC-3 cells. IgG represents a control antibody used for IP. The In represents input control. (B) Expression profile of integrin α3 and β4 in prostate CSCs. Cells stained with antibodies specific to CSC surface markers, CD44-FITC and CD133-PE, and integrin molecules (α3-APC or β4-PE/Cy7) were analysed by FACS. Bar graph indicates relative number of triple-positive ($CD44^+CD133^+α3^+$ or $CD44^+CD133^+β4^+$) CSC population (n=3). *p< 0.05, compared to LNCaP cells. $^{\#}p$< 0.05, compared to PC-3 cells. (C) Cancer stem cell population after silencing *ITGA3* or *ITGB4*. Bar graph indicates relative CSC population ($CD44^+CD133^+$) counts determined from three independent experiments. *p< 0.05, compared to siNT-treated control in each cell line.

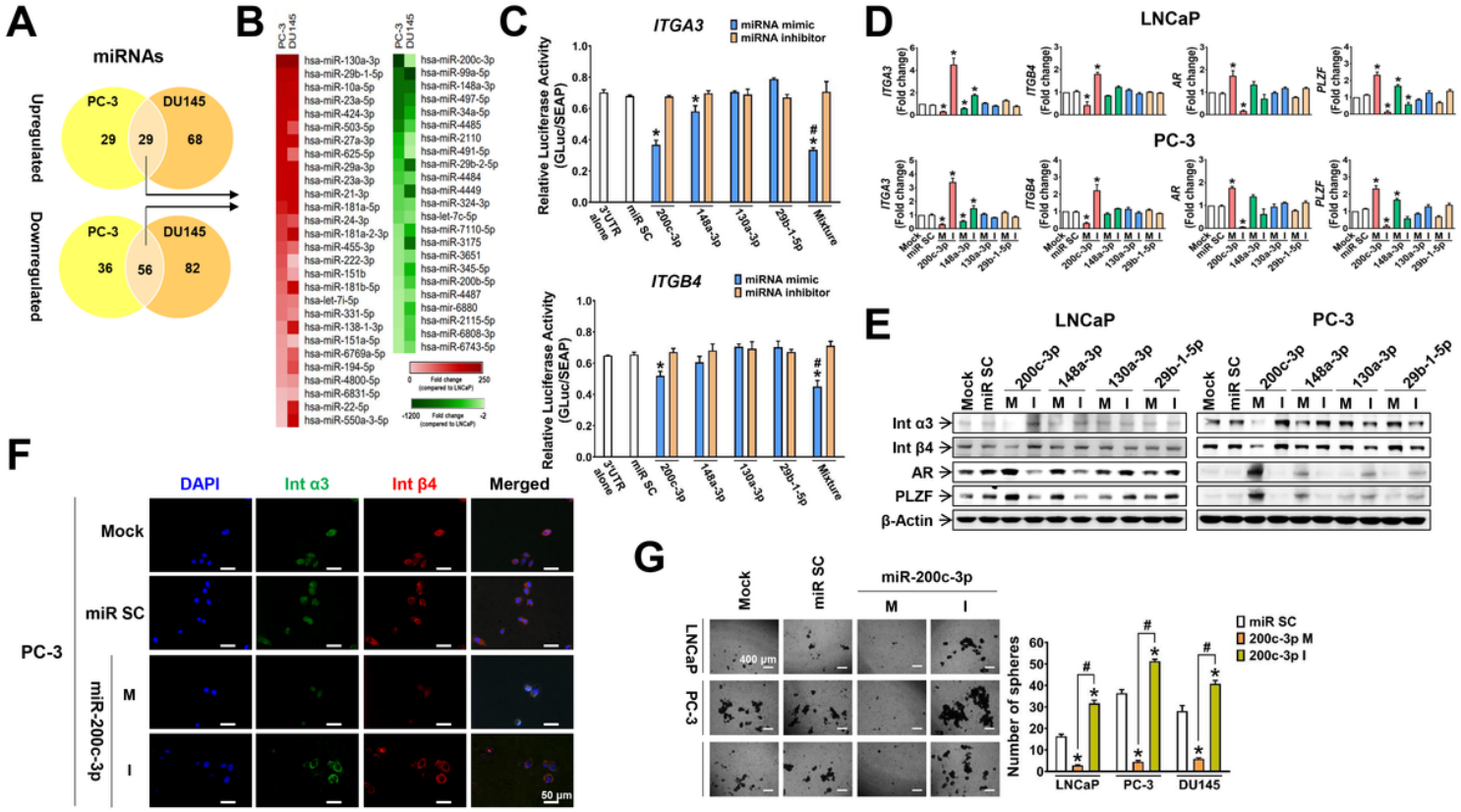

Figure 3

miR-200c-3p, the most significantly decreased miRNA in ARPC cells, downregulates *ITGA3* and *ITGB4* and inhibits PCSC maintenance**.** (A, B) Differential expression of miRNAs was analysed using Affymetrix miRNA 4.0 and presented as Venn diagram (A) showing the number of up- (fold change ≥ 2, $p<0.05$) and downregulated (fold change ≤ 2, $p<0.05$) miRNAs, and heat map (B) showing expression of miRNA that were commonly up- and downregulated in DU145 and PC-3 cells. Heat map was generated using Morpheus software. (C) Luciferase gene reporter assay in HEK-293 cells co-transfected with 3'-UTR constructs (*ITGA3* and *ITGB4*) and miRNA mimic (50 nM) or inhibitor (50 nM) ($n = 3$). *$p<0.05$, compared to scrambled (SC) miRNA-treated group. $^{\#}p<0.05$, compared to miR-200c-3p alone-treated group. (D, E) LNCaP and PC-3 cells treated with four different miRNA mimics or inhibitors were analysed for the expression of integrin α3, β4, AR, and PLZF at mRNA (D) and protein (E) levels. M and I represents mimic and inhibitor, respectively. *$p<0.05$, compared to scrambled (SC) miRNA-treated group. (F) Fluorescence microscopy for integrin α3 (green) and β4 (red) in PC-3 cells. The nucleus was stained with DAPI (blue). Scale bar, 50 μm. (G) Differential opposite effects of miR-200c-3p mimic and inhibitor on tumour spheroid formation. *$p<0.05$, compared to scrambled (SC) miRNA-treated group. $^{\#}p<0.05$, compared to miR-200c-3p mimic-treated group.

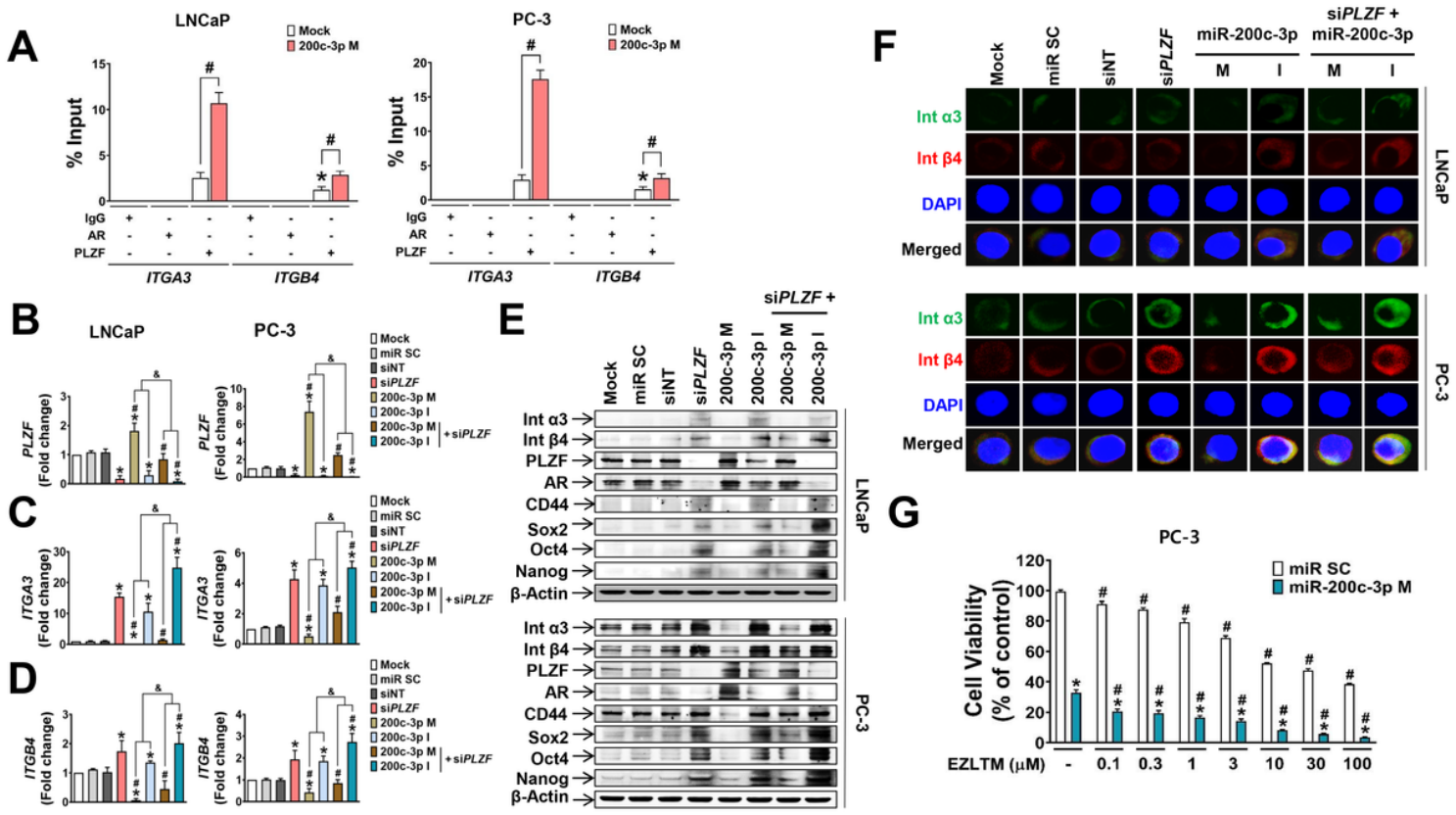

Figure 4

miR-200c-3p upregulates PLZF, which in turn, binds and suppresses the expression of integrin α3β4. (A) ChIP and qPCR validation of the binding of AR or PLZF to *ITGA3* and *ITGB4*. IgG and RNA polymerase II were used as negative and positive controls, respectively. Values were the mean ± SEM from three independent experiments. (B-F) LNCaP and PC-3 cells treated with PLZF siRNA (100 nM), miR-200c-3p (mimic or inhibitor, 50 nM), or both were analysed for mRNA (B-D), protein expression (E), and for co-localisation of integrin α3 and β4 by confocal microscopy (F). *p<0.05, compared to Mock, scrambled (SC) miRNA, or NT siRNA. $^{\#}p$<0.05, compared to PLZF siRNA-treated group. $^{\$}p$<0.05, compared to miR-200c-3p mimic or inhibitor alone-treated group. (G) The viability of cells transfected with miR-200c-3p mimic was measured in the absence and presence of enzalutamide. *p< 0.05, compared to miR-SC-treated control. $^{\#}p$<0.05, compared to vehicle-treated group.

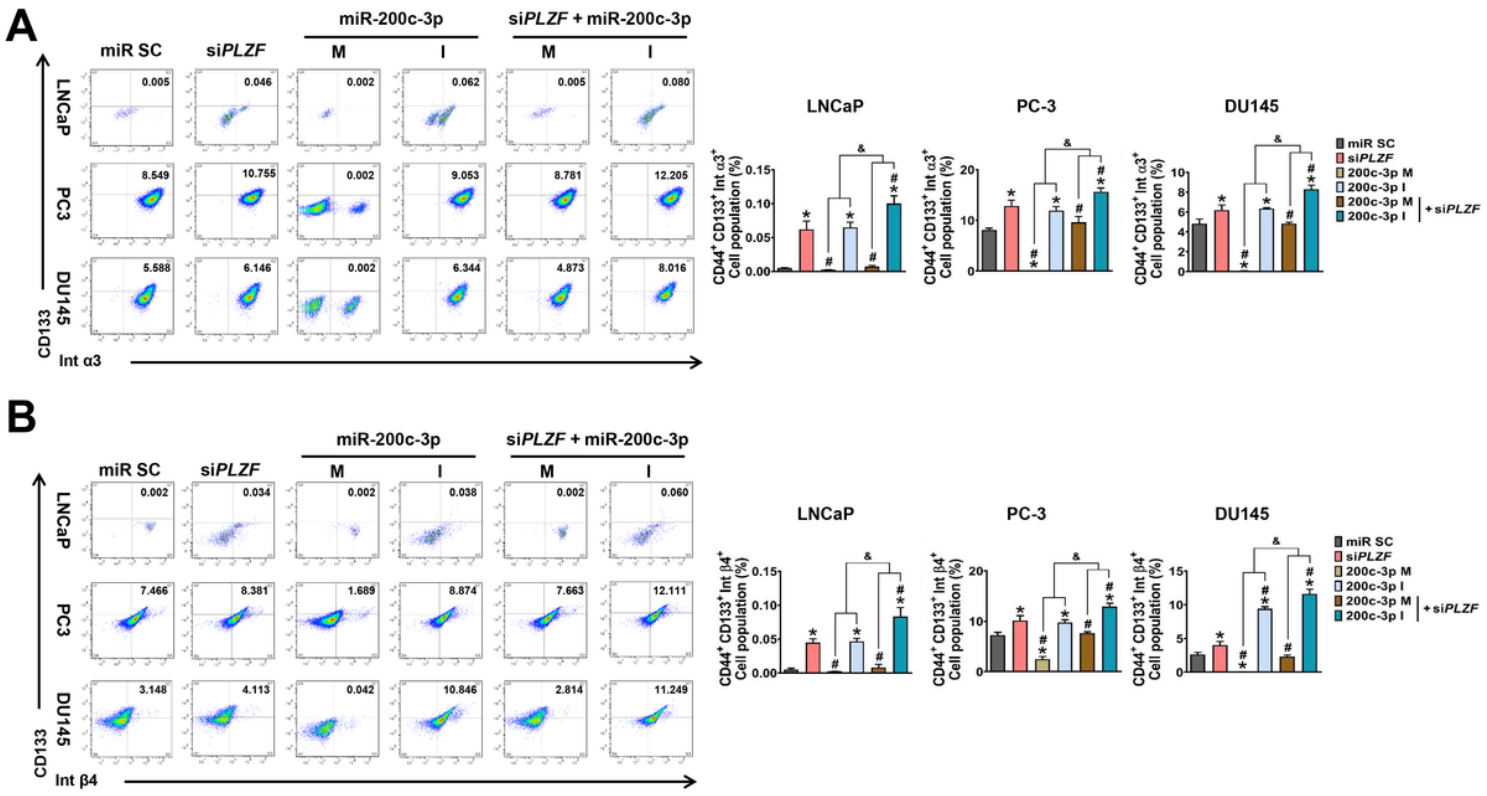

Figure 5

Synergistic effect of miR-200c-3p inhibitor and PLZF siRNA on prostate cancer stem cell increase. Co-treatment with siPLZF and miR-200c-3p inhibitor synergistically enhanced PCSC population that was also positive for α3 (A) or β4 (B) in LNCaP and ARPC (DU145 and PC-3) cells. After treatment with PLZF siRNA (100 nM), miR-200c-3p (mimic or inhibitor, 50 nM), or both, cells were stained with antibodies against CSC surface markers, CD44-FITC, CD133-PE, integrin α3-APC, and integrin β4-PE-CY7, before analysing by FACS. Bar graph indicates relative number of triple-positive ($CD44^+CD133^+\alpha3^+$ or $CD44^+CD133^+\beta4^+$) CSC population (n=3). *p<0.05, compared to Mock, scrambled (SC) miRNA, or NT siRNA. $^{\#}p$<0.05, compared to PLZF siRNA-treated group. $^{\$}p$<0.05, compared to miR-200c-3p mimic or inhibitor alone-treated group.

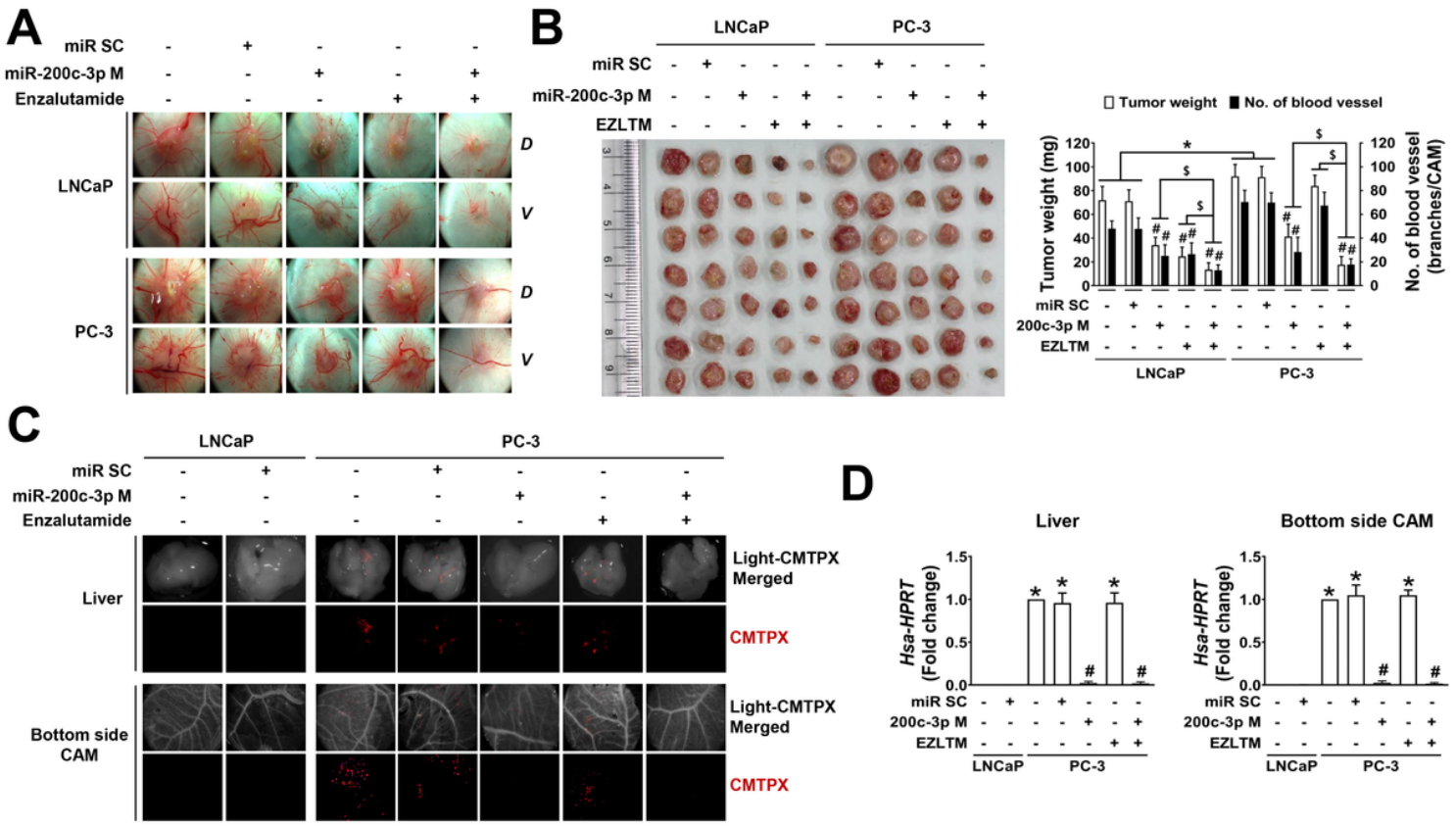

Figure 6

miR-200c-3p mimic treatment restoring androgen sensitivity inhibits tumour growth and metastasis of PC-3 xenografts on CAM. LNCaP and PC-3 cells labelled with CMTPX, a cell-tracker emitting red fluorescence, were implanted on the CAM tissue. Tumour growth and tumour-induced angiogenesis at five days after xenograft are shown in (A). The *D* and *V* represent dorsal and ventral side of cancer-inoculated membrane, respectively. The weight of tumour masses isolated from CAMs and the number of new vessel branches formed on CAM were counted using ImageJ (B). *p<0.05 compared to the vehicle or miR-SC-treated group. $^{\#}p$<0.05 compared to miR-200c-3p mimic- or enzalutamide-treated group. (C, D) For detection of metastasis of xenografts, lower CAM, the opposite site of tumour implants, and liver were collected at day 14, and photographed using stereo and fluorescence microscopy (C). The human cancer cells that had metastasised into the bottom side CAM and liver tissues were quantified based on qPCR for human HPRT (D). *p<0.05, compared to LNCaP cells. $^{\#}p$<0.05, compared to Mock or miR200c-3p mimic-treated group. $^{\$}p$<0.05, compared to miR-200c-3p mimic or enzalutamide alone-treated group.

Supplementary Files

This is a list of supplementary files associated with this preprint. Click to download.

- 1Supplementaryfile.pdf